Available online at www.sciencedirect.com
SCIENCE DIRECT®
ELSEVIER
Nuclear Instruments and Methods in Physics Research B 239 (2005) 347–355
NIM B
Beam Interactions with Materials & Atoms
www.elsevier.com/locate/nimb

A model for ion-bombardment induced erosion enhancement with target temperature in liquid lithium

J.P. Allain [a,*], D.N. Ruzic [b], D.A. Alman [b], M.D. Coventry [b]

[a] *Argonne National Laboratory, Nuclear Engineering, 9700 S. Cass Avenue, Argonne, IL 60439, USA*
[b] *University of Illinois, Urbana-Champaign, IL 61801, USA*

Received 6 April 2004; received in revised form 25 April 2005
Available online 15 July 2005

Abstract

Sputtering does not vary strongly with target temperature for most solid materials. Sputtering yield measurements of liquid lithium self-sputtering for energies of 200–1000 eV at oblique incidence, however, show an enhancement near an order of magnitude as the temperature of the liquid lithium target is increased from near its melting point at 473 K up to about 690 K ($\sim 1.5T_m$) after accounting for thermal evaporation. A new model that couples both the near-surface cascade of the hot liquid metal and the effect of multiple interaction mechanisms on the binding of the emitted particle explains this anomalous erosion enhancement with target temperature. The model, has been validated using a new hybrid computational tool named MD-TRIM (molecular dynamics in transport of ions in matter), at 473 K and 653 K and compared to experimental data. MD-TRIM consists of molecular dynamics and binary collision approximation (BCA) codes, TRIM (transport of ions in matter). The MD-TRIM code was designed to aid in understanding erosion enhancement mechanisms of lithium self-bombardment sputtering at low bombarding energies with a rise in target temperature. MD calculations alone do not show the sputtering enhancement with temperature rise due to an inadequate surface potential model.

PACS: 61.25.Mv; 79.20.Rf

Keywords: Molecular dynamics; Liquid lithium; Sputtering; TRIMSP; MDTRIM

1. Introduction

The number of sputtered particles per incident ion, defined as the sputtering yield, is known not to vary strongly with target temperature for most materials in the solid state [1–9]. The linear theory

* Corresponding author. Tel.: +1 630 252 5184; fax: +1 630 252 3250.
E-mail address: allain@anl.gov (J.P. Allain).

0168-583X/$ - see front matter © 2005 Elsevier B.V. All rights reserved.
doi:10.1016/j.nimb.2005.05.054

of sputtering developed by Sigmund and Thompson relates the physical sputtering yield to the deposited energy at the surface and inversely to the surface binding energy that a sputtered atom must overcome to be emitted [10–12]. This linear regime is characterized by binary collisions between an incident energetic particle and a stationary target atom. When collisions near the surface fail to be of a binary nature or when target atoms are not stationary (e.g. dense cascades developed by heavy-mass, high-energy bombardment) [13,14], the collision is characterized as nonlinear and involves a volume with a high number of moving atoms near the surface. Numerous cases for nonlinear erosion have been studied for materials in the solid and liquid states [15–25]. However, very few studies have been conducted on low-energy (<1 keV) bombardment of liquid metals beyond their melting point.

Experiments in the ion-surface interaction experiment (IIAX) have shown that sputtering from liquid lithium under a variety of bombardment conditions (e.g. variation in incident particle energy (200–1000 eV) and mass (H, D, He and Li)) leads to a nonlinear rise in sputtering as the target temperature is increased beyond the melting point (453 K for Li) [26–28]. These experiments account for evaporation, and the nonlinear rise with temperature is not expected from linear cascade theory. The nonlinear enhancement was also observed in other liquid metals at temperatures beyond their melting point. They include: gallium, tin–lithium and tin [29–31]. Due to the seemingly ubiquitous enhanced sputtering behavior of these liquid metals as their temperature is increased, a model explaining the underlying physics is important to elucidate under what conditions such nonlinear behavior can occur. This behavior appears to be anomalous due to the low bombarding energies involved (e.g. 200–1000 eV). In addition, consideration of these liquid metals as possible advanced plasma-facing components in existing and future fusion devices motivates a thorough understanding on how they erode. This paper presents a model that implements the physics obtained from a molecular dynamics code (MolDyn) combined with a Monte Carlo trajectory code (VFTRIM-3D from TRIM-SP). This hybrid tool (MD-TRIM) simulates multiple interactions of liquid metal surface atoms bombarded by low-energy particles.

2. Description of models

2.1. TRIM-SP and MolDyn

TRIM-SP (transport of ions in matter), based on binary collision approximation (BCA) theory [32], has been used extensively in the simulation of sputtering. In BCA theory, a moving incident particle interacts with a stationary target atom. BCA-based codes such as TRIM-SP have found great success in predicting physical sputtering phenomena for a wide variety of systems and conditions. However, at low incident bombarding energies and in "nonlinear" regimes (i.e. high energy density cascades, surface regions of high atom mobility), collisions are no longer binary, and many-body effects must be accounted for. Nonbinary collisions can be accounted for by the molecular dynamics (MD) code, MolDyn [33]. The many-body nature in MD calculations leads to a more intuitive physical picture and understanding of multiple interaction mechanisms that could exist in liquid metal erosion caused by low-energy ion bombardment [34].

In the MD code the choice of potential for lithium in the liquid state is important. The melting point of lithium is 453 K and very few temperature-dependent potentials exist for lithium. In addition, liquid metals are unique in that at the liquid/vapor interface the atoms are stratified [35]. Since the sputter depth is known to be a few monolayers from the "top" surface [4], applying the proper potential at this interface is very important. Unfortunately, no such potential exists for liquid lithium and only *bulk* interatomic potentials exist [36]. When using this potential, the surface atoms are not properly stratified and are unstable, not maintaining proper cohesion.

In the MD code, a fixed, artificial surface potential barrier must be added due to the instability of lithium atoms at the surface. Its value, 1.67 eV is added to maintain cohesion of the system. Without it, the lattice expands into the free-space

boundary and eventually flies apart. The value is chosen from thermodynamic considerations such that the heat of evaporation and heat of enthalpy are matched. Such a simple model is not adequate for predicting the nonlinear increase in physical sputtering as a function of temperature measured experimentally [26,27]. This is because the effect of this barrier decrease by energetic atoms having multi-body collisions with near-surface atoms is masked. As seen in the results section, running MD alone is not able to predict the experimental data. A more sophisticated surface model is employed in a hybrid code. This model is more appropriate since the bulk Li interatomic potential only properly simulates the multi-body collisions of bulk atoms below the top surface, and not the atoms at the liquid/vapor interface.

One can exploit the strengths of both BCA- and MD-based codes (e.g. TRIM-SP and MolDyn) in a hybrid tool to study atomistic phenomena such as physical sputtering of liquid metals. This tool addresses the drawbacks of the MD simulations: massive computation time required for sufficient statistics and a fixed global surface potential. Such hybrid tools have been used for solids [34,37,38]. This paper introduces a similar tool for liquids: MD-TRIM, a hybrid of the BCA-based TRIM code with the formulation utilized in VFTRIM-3D [39] (which differs from TRIM-SP by adding a three-dimensional fractal surface model to account for surface roughness effects) including physical mechanisms obtained from MolDyn [33]. The goal of the hybridization is to retain the important "physics" from the MD simulations while minimizing computation time by use of the TRIM simulation structure and addressing the lack of an adequate potential for the liquid/vapor interface.

2.2. MD-TRIM

MD-TRIM incorporates two important mechanisms believed responsible for enhanced sputtering in liquid metals with an increase in system temperature [26]. The first mechanism is the many-body nature of the near-surface collision cascade characterized by the energy and angular recoil distribution. The second mechanism is the relative binding of the emitted particle with neighboring surface atoms before emission. A similar description of multiple interactions near the surface leading to enhancement in sputtering exists in the literature. These studies explain how multiple interactions that lead to nonlinear events are atypical, such as the sputtering of a near-surface atom [34,37,38,40–42]. This particular effect cannot be simulated with exiting liquid lithium MD potentials and thus the need for MD-TRIM.

In MD-TRIM both mechanisms described above are obtained from 100 MolDyn flights at two temperatures: 473 K and 653 K. The lithium cell in MolDyn consists of 2700 atoms that are equilibrated at each temperature using a Berendsen thermometer [43]. The bottom boundary is fixed, while side boundaries are periodic, and the top boundary free [33]. The equations of motion for each individual lithium atom are calculated over a series of 0.2-fs time steps. The potential energy and force between a pair of lithium atoms are calculated from their separation distance according to a two-body interatomic potential for liquid lithium developed by Canales and Gonzalez [36,44,45].

The target surfaces for the MD simulations were prepared by gradually raising the temperature of a BCC lithium lattice from 0 K to the desired temperature above the melting point. The surfaces were then allowed to equilibrate at the desired temperature until there were no temperature fluctuations, typically for about 100 ps. Fig. 1 shows the radial distribution functions at 0, 473 and 653 K, demonstrating that the surfaces have been melted. The absolute order of the BCC lattice is gone, yet the short-range order, typical of liquids, is evident. The energy of the incident Li atom is 100 eV and is incident at 45°.

2.3. Differences between MD-TRIM and VFTRIM-3D

The principal difference between MD-TRIM and VFTRIM-3D is how MD-TRIM handles the creation of primary knock-on atoms (PKA). VFTRIM-3D uses the BCA with additional "soft" collisions, which change the energy loss term but not the particle's direction. To model all collision

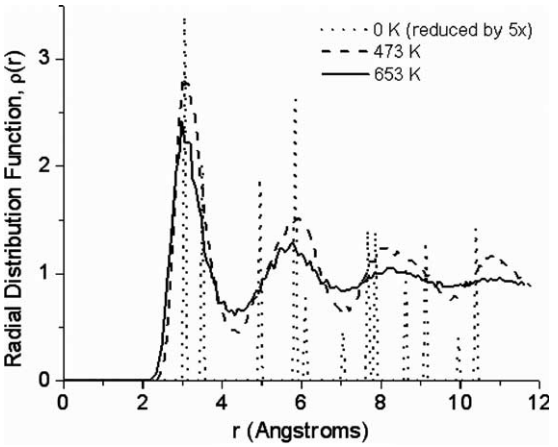

Fig. 1. Radial distribution function from MolDyn simulations at 0 K, 473 K and 653 K.

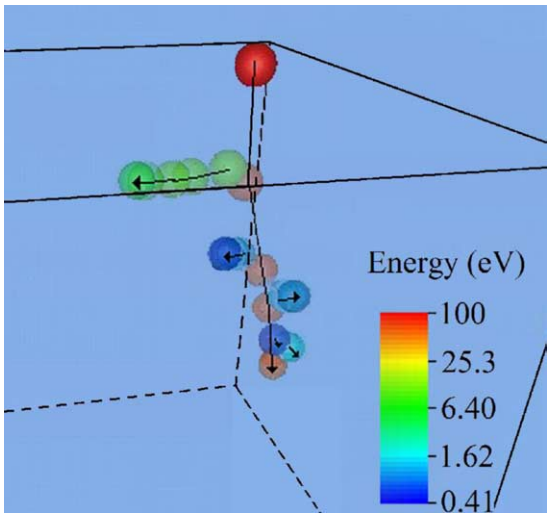

Fig. 2. A composite image of six frames taken from a movie showing a lithium atom incident on a liquid lithium surface. The incident atom is shown in red (the highest energy in the system), and various primary knock-on atoms with lower kinetic energy are generated during the transit of the incident atom. The arrows show the direction of movement of each atom. The frames represent times of 5, 21, 37, 45, 57 and 61 fs into the simulation. (For interpretation of colours in this figure legend, the reader is referred to the web version of this article.)

interactions, MD-TRIM uses an MD-derived PKA creation module to generate both energy and direction changes based on all partners involved in primary collisions. For higher-generation collisions, MD-TRIM resorts to the BCA mechanism supplied by VFTRIM-3D. The method of determining the recoil angle, energy transferred, and scattering angle sets MD-TRIM apart from standard TRIM codes such as VFTRIM-3D.

VFTRIM-3D determines the impact parameter randomly (within a certain range) and uses that impact parameter with Biersack's "magic" formula [46] to determine the scattering angle. Once the scattering angle is determined, the amount of energy transferred to each recoil is then calculated. The recoil angle is then determined via conservation of energy and momentum. Another random number determines the azimuthal scattering angle. MD-TRIM, in contrast, generates primary recoil interaction information from a table generated from MolDyn simulation results. An example of PKA generation in the MD code is shown in Fig. 2, showing large angle recoil generation, near the top surface, and the generation of several PKAs in the same collision (i.e. through the many-body nature of molecular dynamics). The recoil angle, fractional energy transferred, and scattering angle are listed for each primary collision from 100 MolDyn flights. This method was chosen as an alternative to fitting distributions for each of these quantities in order to prevent artificial coupling of the three parameters. While this method allows only discrete angles and energies to be generated, sufficient statistics overcome this obstacle and approach continuous distributions.

VFTRIM-3D also requires input of the surface binding energy, which can be determined in a number of ways as the temperature of the system varies. One way is to correlate the surface binding energy to the surface free energy of the system through the use of surface tension as a function of temperature. This approach has shown only a marginal increase of the surface binding energy with temperature. A different method is to identify those particles in MolDyn which sputter and to determine the minimum energy that those particles need to overcome the surface energy barrier. This method is applied in MD-TRIM, where the minimum energy is denoted as the minimum escape energy (MEE), and sets MD-TRIM apart from BCA models such as VFTRIM-3D. The MEE is defined

as the change in potential energy of the particle to be emitted (sputtered) as the normal component of the particle's position crosses the surface. In VFTRIM-3D a fractal surface of dimension = 2.00 (smooth surface) is used.

3. Results and discussion

3.1. Recoil angular distribution

Fig. 3 shows the recoil angular distribution for the PKA population plotted versus the recoil angle. The plot shows the effect on the recoil angular distribution when multiple interactions are accounted for. For the case of the BCA-based simulation, recoil angles cannot exceed 90° due to simple conservation of momentum. The PKA distributions found from MolDyn differ greatly from those seen in VFTRIM-3D. MolDyn showed *net* recoil angles up to 160° as a consequence of multi-body collisions, with the majority of the collisions producing PKA motion at nearly right angles from the initial trajectory. Since several atoms are being struck at once in such an interaction, the PKA is defined as the recoil atom which receives the most energy.

3.2. Recoil fractional energy distribution

Fig. 4 shows the recoil fractional energy distribution versus the ratio of the kinetic energy of the PKA created to that of the incident particle prior to the collision for VFTRIM-3D and MolDyn runs at 473 and 653 K. Note that the peak shifts from lower energy transfer per collision in the BCA-based VFTRIM-3D results to higher values in the MolDyn results. In addition, the fraction of energy transfer per collision is higher at 653 K than at 473 K. As a consequence, the deposited energy density is higher at 653 K. Coupling of the lateral motion of energetic recoils near the surface to the manner in which atoms near the surface are bound (e.g. the MEE) defines the key mechanisms responsible for enhanced erosion as the system temperature is increased.

3.3. Minimum escape energy

In addition to the PKA distribution, we also determined the MEE needed to overcome the potential well of the sputtered particle right before ejection from the liquid metal surface, using 100 flights from MolDyn. Figs. 5 and 6 show the temporal dependence of the emitted particle's total,

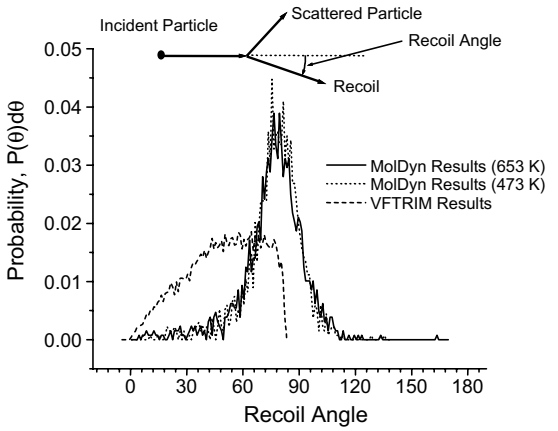

Fig. 3. The recoil angular distribution obtained from 100 MolDyn flights that resulted in about 1200–1500 recoils. In VFTRIM no recoil angles can exceed 90° due to the use of the binary collision approximation. In MolDyn multi-body effects allow the *net* recoil angles to exceed 90°; recoils in general are along the surface.

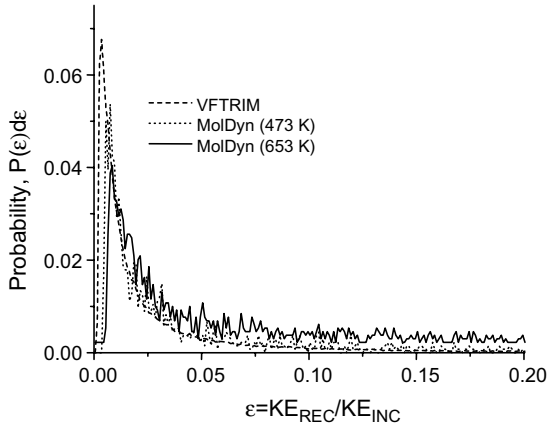

Fig. 4. Recoil energy distribution obtained from 100 MolDyn flights that resulted in about 1200–1500 recoils. Note a larger amount of the incident energy is transferred to PKAs (primary knock-ons) as the temperature of the system increases. The symbol ε is the fraction of its energy the incident ion imparted to the recoil.

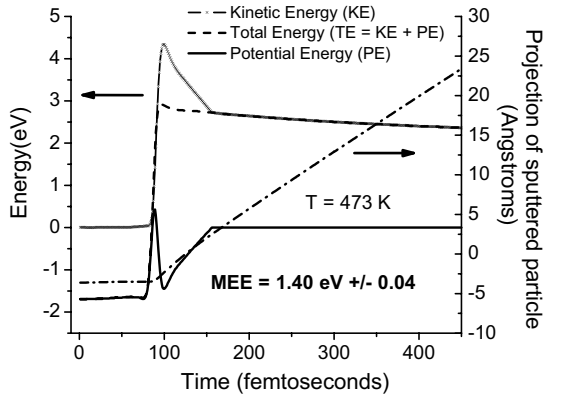

Fig. 5. The energy–time evolution of a sputtered lithium particle plotted along with its projected trajectory along the perpendicular direction to the surface at 473 K. The total energy consists of the kinetic and potential energies. The minimum escape energy (MEE) is determined by the energy well in the potential just before leaving the surface at 125 fs.

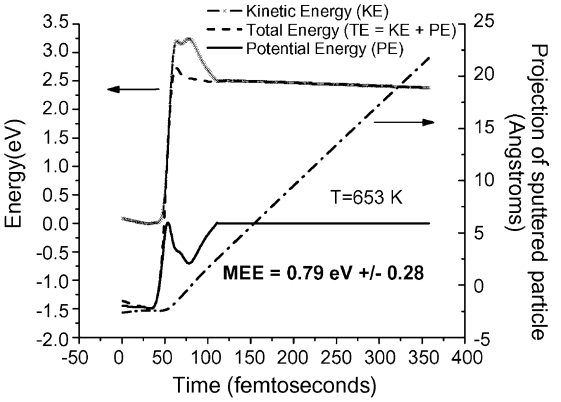

Fig. 6. The energy–time evolution of a sputtered lithium particle plotted along with its projected trajectory along the perpendicular direction to the surface at 653 K. The total energy consists of the kinetic and potential energies. The minimum escape energy (MEE) is determined by the energy well in the potential just before leaving the surface at 82 fs.

kinetic and potential energy for 473 and 653 K, respectively. Note that MEE is defined as the change in potential energy of the particle to be emitted (sputtered) as the normal component of the particle's position crosses the surface. This energy is found to be a sensitive function of temperature. For example, the average MEE is equal to 1.4 eV at 473 K and 0.79 eV at 653 K. These values were obtained by averaging over all sputtered atoms, the MEE in the MD simulation at each temperature.

This temperature dependent behavior is analogous to the multiple interaction of near-surface atoms studied by Jakas et al. [34,37,38,40]. An atom near the surface only needs to be given about 0.79 eV of *kinetic energy* or more to be emitted if the surface is at 653 K, not the 1.67 eV – the "surface binding energy" – normally assumed. The nonbinary collisions with neighbors of the atom to be sputtered weaken their grip on the atom. As Figs. 5 and 6 show, the degree to which that grip can be weakened varies with temperature.

3.4. Sputtering results from MD-TRIM

With both mechanisms implemented in MD-TRIM, the code runs for 10^4 flights to obtain the sputtering yield at both 473 and 653 K. These results are presented in Table 1 and compared to estimated experimental self-sputtering data and MD results from liquid lithium at both temperatures. The experimental results are estimates because experiments to date in our IIAX apparatus have only been done at this energy and temperatures with lithium incident on lithium targets treated with deuterium or helium incident on non-treated targets [47,48]. The estimated experimental yields are 0.80 ± 0.2 Li/ion at 473 K and 1.20 ± 0.3 Li/ion at 653 K. Lithium sputtering experiments by Allain have shown that in the solid state and temperatures near Li melting (453 K) the D-saturated surface will sputter a factor of about 4–5 times less than a pure Li or non-D-treated surface when bombarded by He or D ions at energies between 100 and 1000 eV [47,48]. Li self-sputtering data taken for temperatures between 473 K and 683 K (above melting point) on D-treated surfaces shows yields of 0.2 Li/ion (200 eV Li^+) and 0.9 Li/ion (300 eV Li^+), respectively [27]. Data also shows an apparent shift of the maximum of the energy-dependent sputter yield to lower energies from 700 eV to about 300 eV [49]. The self-sputter yield for a pure Li target at 473 K was therefore estimated to be about 0.8 Li/ion for an incident energy of 200 eV. At 100 eV this would be an uppermost limit and thus we used this value to compare

Table 1
Temperature dependence of MD-derived MEE (minimum escape energy) and comparison of lithium sputtering yield between MD-TRIM and experimental data

Temperature (K)	MD-derived MEE (eV)	Sputtering yield (particles/ion)		
		MolDyn	MD-TRIM	Experiment (estimated)
473	1.40	0.20	0.75	0.80 ± 0.20
653	0.79	0.26	1.29	1.20 ± 0.30

Case for 100 eV Li on liquid Li at 45° incidence.

Table 2
Lithium sputtering yield results from MD-TRIM compared to VFTRIM

MEE (eV)	Sputtering yield (particles/ion)		
	VFTRIM (MEE is SBE in TRIM)	MD-TRIM (473 K)	MD-TRIM (653 K)
0.79	0.84	1.18	1.29
1.40	0.49	0.75	0.81
1.68	0.42	0.64	0.70

to MD-TRIM simulations at 473 K. For the case at 653 K, the effect of D-saturation is lessened since more D atoms diffuse to the bulk and thus the Li sputter yield approaches that of a pure Li surface [47,49]. The estimated Li self-sputter yield at 653 K was therefore about 1.2 Li/ion for 300 eV also an upper-most limit. The uncertainty in these estimates coupled to the uncertainty in the experiments yield errors of ±20–30%.

Table 1 shows good agreement between MD-TRIM calculations and the estimated experimental data. The MD results are from approximately 700 flights run at each temperature with the timestep and the potentials described previously. The results are five times lower than both the experiment and the MD-TRIM simulation and show only a modest increase with target temperature. The MD simulation shows the average energy of the sputtered atoms rises slightly (2.9–3.4 eV) instead of the experimentally noted decrease of average energy. MD-TRIM does show a decrease of sputtered atom average energy.

Table 2 shows a comparison of MD-TRIM results versus the standard VFTRIM-3D (BCA-based) code for three MEEs. In VFTRIM-3D, MEE is simply the standard surface binding energy. Note that VFTRIM-3D with the standard surface binding energy (SBE) of 1.68 eV, underestimates the experimental data and has no temperature dependence. Merely changing the SBE from 1.4 eV down to 0.79 eV increases the sputtering yield as expected, but not to the extent seen in the estimated experimental values. In addition, Table 2 shows that using the MD-derived PKA distributions at the two temperatures using the standard heat of sublimation (1.68 eV) in MD-TRIM increases the sputtering yield as expected, but also not to the degree seen in the estimated experimental values. It is a combination of the MEE values extracted from the MD simulations at each temperature *coupled* to the MD-derived PKA distributions that a realistic prediction is made for liquid Li sputtering at 100 eV for temperatures at 473 and 653 K. This particular combination is what makes up the Allain–Ruzic model implemented in MD-TRIM.

4. Conclusions

In summary, two mechanisms are responsible for the yield enhancement measured with a rise in system temperature for liquid lithium. The first is the near-surface cascade described by the generation of primary recoils that move laterally, transferring their energy more efficiently at higher system temperatures to mobile atoms near the surface. The second is the nature of bonding of the

emitted lithium particle with respect to its nearest target atom neighbors and is defined by the MEE. Coupling of these two mechanisms forms the basis of the Allain–Ruzic model implemented in MD-TRIM, explaining the erosion of hot liquid metals. These mechanisms are also expected in hot solids and frozen condensed-gas solids at low ion impact energies, however, they are more conspicuous in the liquid state. This is due to higher mobility of atoms as the thermodynamic state rises above the melting temperature of the material on the time scale characteristic of physical sputtering (0.5–1.0 ps).

Another important result of the Allain–Ruzic model is the ability to predict the energy and angular distributions of the sputtered particles from a liquid metal surface as a function of system temperature, incident particle mass and energy, and surface chemical state using MD-TRIM. For example, according to this model one would expect that as the system temperature is increased from near melting up to temperatures where evaporation begins to dominate erosion for lithium ($\sim$700 K), more particles would be emitted and the energy distribution of sputtered particles would shift towards *lower* energies. This phenomenon has been seen for frozen condensed-gas solids as well [50]. This model not only provides a computational tool, but also a straightforward way of thinking about low energy (10–1000 eV) particle collisions with a liquid metal as a function of temperature without resort to semi-empirical fitting parameters typical of nonlinear erosion models, such as thermal spikes, or models based on adatom formation on liquid surfaces.

The failure of the MD code alone to adequately predict sputtering yields for a liquid metal is namely due to the lack of an adequate surface potential model. This is due to the unique behavior liquid metals possess at the liquid–vapor interface. The only existing potentials for liquid metals, in particular alkali metals in the liquid state, only predict the characteristics of the liquid–vapor interface but lack the ability to predict physical sputtering [47–49]. MD-TRIM addresses this shortcoming by utilizing the nonbinary collision capabilities of MD simulations whilst including the temperature-dependent behavior of the MEE due to nonbinary collisions near the surface ultimately increasing the probability of sputtering as evidenced in temperature-dependent liquid Li sputtering measurements. Future work will focus on implementing liquid Li surface potentials recently developed using ab initio molecular dynamics methods [51] to describe the low-energy sputtering of Li in the liquid state.

Nonlinear erosion due to nano-bubble formation in liquid metals remains an open question and is the subject of upcoming work. For the conditions of low flux on the experiments referred to in this paper, however, formation of bubbles in liquid lithium from self-bombardment is not expected. Surfaces of liquid metals are also known to form a layered structure at the liquid/vapor interface [35,52,53] as stated earlier. The effect of this stratified layer to the sputtering yield as a function of temperature may be important, and further atomistic simulation studies are needed to address this issue.

Acknowledgements

The authors would like to acknowledge Martin Nieto and Huatan Qiu for assistance with data analysis, R. Averback for supplying the MolDyn code and L.E. Gonzalez for supplying liquid Li potentials at various temperatures.

References

[1] P. Sigmund, Phys. Rev. 184 (2) (1969) 383.
[2] P. Sigmund, Appl. Phys. Lett. 25 (3) (1974) 169.
[3] P. Sigmund, in: N.H. Tolk (Ed.), Sputtering Processes: Collision Cascades and Spikes, Academic Press, New York, 1977.
[4] P. Sigmund, N.Q. Lam, Matematisk-fysiske Meddelelser Det Kongelige Danske Videnskabernes Selskab 43 (1993) 255.
[5] P. Sigmund, M. Szymonski, Appl. Phys. A: Solids Surf. 33 (1984) 141.
[6] R. Behrisch, W. Eckstein, Nucl. Instr. and Meth. B 82 (1993) 255.
[7] K. Besocke et al., Radiat. Effects 66 (1982) 35.
[8] J. Bohdansky et al., Nucl. Instr. and Meth. B 18 (1987) 509.
[9] J. Bohdansky, J. Roth, Nucl. Instr. and Meth. B 23 (1987) 518.

[10] P. Sigmund, in: R. Behrisch (Ed.), Sputtering by Particle Bombardment I, Springer-Verlag, Berlin, 1981.
[11] M.W. Thompson, Vacuum 66 (2002) 99.
[12] M.W. Thompson, Phys. Rep. 69 (4) (1981) 335.
[13] R.S. Nelson, Philos. Mag. 11 (1965) 291.
[14] M.W. Thompson, R.S. Nelson, Philos. Mag. 7 (1962) 2015.
[15] H.H. Andersen et al., Phys. Rev. Lett. 80 (24) (1998) 5433.
[16] T.J. Colla et al., Phys. Rev. B 62 (12) (2000) 8487.
[17] E.M. Bringa, R.E. Johnson, Nucl. Instr. and Meth. B 143 (4) (1998) 513.
[18] E.M. Bringa, R.E. Johnson, L. Dutkiewicz, Nucl. Instr. and Meth. B 152 (1999) 267.
[19] L.B. Begrambekov et al., Sov. Atomic Energy 64 (3) (1988) 263.
[20] E.M. Bringa, R.E. Johnson, Phys. Rev. Lett. 88 (16) (2002) 165501.
[21] H.P. Cheng, J.D. Gallaspy, Phys. Rev. B 55 (4) (1997) 2628.
[22] Kristin D. Krantzman et al., Nucl. Instr. and Meth. B 180 (2001) 159.
[23] A. Delcorte, B.J. Garrison, J. Phys. Chem. B 104 (2000) 6785.
[24] E.M. Bringa, R.E. Johnson, M. Jakas, Phys. Rev. B 60 (22) (1999) 15107.
[25] J. Roth, W. Möller, Nucl. Instr. and Meth. B 7/8 (1985) 788.
[26] J.P. Allain, M.D. Coventry, D.N. Ruzic, J. Nucl. Mater. 313–316 (2003) 645.
[27] J.P. Allain, Ph.D. Thesis, University of Illinois at Urbana-Champaign, 2001.
[28] J.P. Allain et al., Fus. Eng. Des. 72 (1–3) (2004) 93.
[29] R.W. Conn et al., Nucl. Fus. 42 (2002) 1060.
[30] M.D. Coventry, J.P. Allain, D.N. Ruzic, J. Nucl. Mater. 335 (1) (2004) 115.
[31] R.P. Doerner et al., J. Nucl. Mater. 313–316 (2003) 385.
[32] J.P. Biersack, W. Eckstein, J. Appl. Phys. A 34 (1984) 73.
[33] D.A. Alman, D.N. Ruzic, J. Nucl. Mater. 313–316 (2003) 182.
[34] R.P. Webb, D.E. Harrison Jr., M.M. Jakas, Nucl. Instr. and Meth. B 15 (1986) 1.
[35] J. Penfold, Rep. Prog. Phys. 64 (2001) 777.
[36] M. Canales, L.E. Gonzalez, J.A. Padro, Phys. Rev. E 50 (5) (1994) 3656.
[37] M.M. Jakas, D.E. Harrison Jr., Nucl. Instr. and Meth. B 14 (1986) 535.
[38] M.M. Jakas, D.E. Harrison Jr., Phys. Rev. Lett. 55 (17) (1985) 1782.
[39] D.N. Ruzic, Nucl. Instr. and Meth. B 47 (1990) 118.
[40] R.P. Webb et al., Nucl. Instr. and Meth. B 112 (1996) 99.
[41] D.N. Ruzic, IEEE Trans. Plasma Sci. 24 (1) (1996) 81.
[42] D.N. Ruzic, American Vacuum Society, New York, 1991.
[43] H.J.C. Berendsen et al., J. Chem. Phys. 81 (8) (1984) 3684.
[44] L.E. Gonzalez, D.J. Gonzalez, M. Canales, Zeit. Phys. B 100 (1996) 601.
[45] L.E. Gonzalez et al., J. Phys.: Condens. Matter 5 (1993) 4283.
[46] J.P. Biersack, L.G. Haggmark, Nucl. Instr. and Meth. 174 (1980) 257.
[47] J.P. Allain, D.N. Ruzic, in: A. Hassanein (Ed.), NATO Science Series: Hydrogen and Helium Recycling at Plasma Facing Materials, Vol. 54, Kluwer Academic Publishers, Dordrecht, 2002, p. 73.
[48] J.P. Allain, D.N. Ruzic, Nucl. Fus. 42 (2002) 202.
[49] J.P. Allain, M.D. Coventry, D.N. Ruzic, J. Appl. Phys., submitted for publication.
[50] R.E. Johnson, M. Pospieszalska, W.L. Brown, Phys. Rev. B 44 (14) (1991) 7263.
[51] D.J. González, L.E. González, M.J. Stott, Phys. Rev. Lett. 92 (2004) 085501.
[52] S.A. Rice, J. Non-Cryst. Solids 205–207 (1996) 755.
[53] P.S. Pershan, Physica A 231 (1996) 111.